

Effects of grain size distribution on the initial small strain shear modulus of calcareous sand

Effets de la Distribution des Grains sur la Module de Cisaillement Initial du Sable Calcaire

P. H. Ha Giang^{*1}, P. Van Impe², W.F. Van Impe², P. Menge³, and W. Haegeman¹

¹ Ghent University, Ghent, Belgium

² Ghent University, AGE Advanced Geotechnics Engineering Bvba, Ghent, Belgium

³ Dredging International, Zwijndrecht, Belgium

^{*} Corresponding Author

ABSTRACT: The soil's small strain shear modulus, G_{\max} or G_0 , is applied in dynamic behavior analyses and is correlated to other soil properties (density and void ratio) for predicting soil dynamic behavior under seismic loadings such as earthquakes, machinery or traffic vibrations. However, for calcareous sands, selecting representative samples for the field conditions is difficult; therefore, almost all measured soil parameters (post-seismic properties) do not reflect exactly the soil state before seismic loading. In some cases of dynamic loading, a change in grain size distribution (GSD) of soils, especially for calcareous sands might occur. Moreover, many of these sand types behave differently from silica sands owing to their mineralogy, particle characterization, soil skeleton, and the continuous changing of particle size. For this reason, a series of isotropic consolidation tests in ranges of confining pressure from 25 to 300 kPa as well as bender element measurements on a calcareous sand and on a reference silica sand were performed in this study. The effects of differences in gradation and in the type of material on the soil's small strain shear modulus, G_{\max} , are discussed.

RÉSUMÉ: La module de cisaillement initial, G_{\max} ou G_0 , est appliquée dans des analyses du comportement dynamique du sol sous sollicitations sismiques tels que les tremblements de terre, des machines ou des vibrations de la circulation et est corrélée à d'autres propriétés du sol (densité et indice des vides). Pourtant, pour les sables calcaires, la sélection des échantillons représentatifs des conditions sur le terrain est difficile; par conséquent, la quasi-totalité des paramètres mesurés (post-sismique propriétés) ne reflète pas exactement l'état du sol avant le chargement sismique. Dans certains cas de chargement dynamique, un changement dans la répartition de la taille des grains, en particulier pour les sables calcaires, peuvent se produire. En outre, beaucoup de ces types de sable se comportent différemment des sables siliceux en raison de leur minéralogie, la caractérisation des particules, la squelette du sol et l'évolution continue de la taille des particules. Dans cette étude une série d'essais de consolidation isotrope dans des gammes de pression de confinement de 25 à 300 kPa, ainsi que des mesures de propagation d'ondes de faible amplitude sur un sable calcaire et un sable de silice de référence ont été effectuées. Les effets des différences de gradation et du type de matériau à la module de cisaillement, G_{\max} , sont discutés.

1. INTRODUCTION

The shear modulus at small strain, G_{\max} , which is typically 10^{-4} or less, is one of the basic soil parameters. It is determined from the shear wave velocity (V_s), which is measured directly in-situ or in the lab ($V_s = \sqrt{G_{\max} / \rho}$). In the lab, it is conducted by wave propagation velocity measurements or the very precise laboratory

measurement of stress and strain in soil samples (Towhata 2008). Beside the resonant column method, the bender element method developed by Shirley & Hampton in 1978 (cited in (Maheswari et al. 2008)) is one of the laboratory methods to obtain G_{\max} by measuring the velocity of the shear wave propagating through the sample. The

laboratory experiments indicate that the bender element measurements of G_{\max} are comparable to the corresponding resonant column measurements, with differences of less than 10% (Yang & Gu 2013). This method has generated intensive studies from many researchers in the past (Bellotti et al. 1996, Santamarina & Fratta 2005, Builes et al. 2008).

However, sampling undisturbed calcareous sands is difficult. Moreover, all measured soil parameters (post-seismic properties) do not reflect exactly the soil state before shaking. Indeed, after seismic loading or vibrating compaction there may be a change in grain size distribution (GSD) of soils, especially for calcareous sands. Based on the literature, various parameters affect the small strain shear modulus such as stress state, material characteristics including void ratio, particle size, particle shape, gradation, fabric, cementation, etc., and strain level (Bui et al. 2007). Hyodo et al. (1996) investigated crushable sands, which have lower grain hardness, larger intra-granular porosity, a wider range of grain shapes, and more complex structural arrangements. He concluded that their mineralogy, particle shape, soil skeleton, and high void ratios contribute to their compressibility. In addition, a number of studies also showed that the compressibility of calcareous sands is greater than silica sands (Datta et al. 1982, Hyodo et al. 1996, Sandoval & Pando 2012).

This study uses laboratory data obtained from reconstituted samples to predict the variation of G_{\max} for calcareous sands. A common empirical equation for small strain shear modulus G_{\max} as a function of void ratio e and mean effective confining pressure p' , first proposed by Hardin & Richart (1963) (cited in Santos & Gomes Correia 2000) is as follow:

$$G_{\max} = A * F(e) * \left(\frac{p'}{p_a}\right)^n \quad (1)$$

where e is void ratio, the empirical void ratio function $F(e) = B \left(\frac{a-e}{1+e}\right)^2$ proposed by Iwasaki & Tatsuoka (1977) ($a = 2,17$ and $2,79$ for round and angular grained sands, respectively) or $F(e) = e^{-B}$ proposed by Lo-Presti (1998) (cited by (Santos & Gomes Correia 2000), p' is mean effective stress, p_a is a reference pressure of 100 kPa (the

atmospheric pressure), and A , B , and n are material constants.

Iwasaki & Tatsuoka (1977) concluded that shear moduli decrease with increasing C_u . However, they considered only the effects of C_u on the parameter B (proposed by Iwasaki & Tatsuoka (1977)) of the void ratio function used in the equation (1). B increases when C_u decreases. In addition (Menq et al. 2003) showed that the exponent n of the confining pressure increases with increasing C_u . Wichtmann & Triantafyllidis (2009) also investigated the influence of GSD curves on the small strain shear modulus G_{\max} of quartz sand. They confirmed an increase of the exponent n with increasing C_u and proposed a correlation between C_u and the material constants A , B , and n where the effects of particle characteristics as particle angularity on these parameters are not mentioned yet.

The objective of this study is to determine G_{\max} by the equation (1) for calcareous and silica sands with different void ratios, densities, GSD under saturated condition so G_{\max} can be predicted for dynamic soil applications for these materials.

2. EXPERIMENTAL PROGRAM

A total number of 12 isotropic consolidation tests are considered in this study. The experiments are performed on four materials with three different gradations and are prepared at three initial relative densities (15%, 40%, 60%) and finally consolidated at confining pressures 25, 50, 75, 100, 125, 150, 175, 200, 225, 250, 275, 300 kPa. Volume change is measured during testing and bender elements tests are excited by single sinusoidal pulse waves at each confining pressure.

2.1. Test materials

There are two original materials, Mol sand and Sarb sand, used in the experiments. Mol sand, a silica sand, is taken from a municipality located in the Belgian province of Antwerp; and Sarb sand, a calcareous sand, is obtained from an artificial island in Abu Dhabi, United Arab Emirates.

The main purpose of this work is to find out the effects of different GSD on the initial shear modulus of calcareous sand; silica sand is taken for comparison. Sarb sand is crushed on a vibrating table following the ASTM D 4254-00 to have a different crushable material with finer GSD curve, afterward called VSarb sand. In the concept of this work, Sarb sand was also used to match the GSD of the silica sand by copying the GSD of Mol sand. SarbMol sand has the same shape, angularity as Sarb sand but the GSD of Mol sand. This is to see the effects on G_{\max} of differences in particle morphology, type of material and GSD.

The physical properties of the studied sands, determined according to ASTM and Japanese Geotechnical Society standards, are summarized in

Table 1 and the GSD curves are depicted in Figure 1. Sarb sand is separated into 13 grain size fractions with 12 grain size fractions bigger than $63\mu\text{m}$ as shown in Figure 2. The tests are performed in the Geotechnical lab of Ghent University. According to ASTM D2487-10, the GSD curves indicate clearly that all materials are termed as sandy-grained soil. Sarb sand is the only well-graded sand, whereas VSarb, SarbMol and Mol sand are classified as poorly-graded sands.

Table 1. Physical properties of the studied sands

| Physical Properties | Mol | Sarb | VSarb | SarbMol | Standard |
|--|-------|-------|-------|---------|---------------|
| Specific gravity, G_s | 2,637 | 2,787 | 2,787 | 2,787 | ASTM D 854-06 |
| Mean grain size, D_{50} (mm) | 0,167 | 0,73 | 0,425 | 0,167 | ASTM D 422-63 |
| Coefficient of uniformity, $C_u = D_{60}/D_{10}$ | 1,44 | 3,46 | 5,429 | 1,44 | ASTM D 422-63 |
| Coefficient of gradation, $C_c = \frac{(D_{30})^2}{(D_{10} * D_{60})}$ | 0,93 | 1,12 | 0,809 | 0,930 | ASTM D 422-63 |
| Max. void ratio, e_{\max} | 0,93 | 1,33 | 0,956 | 1,340 | JIS A 1224 |
| Min. void ratio, e_{\min} | 0,581 | 0,903 | 0,508 | 0,843 | JIS A 1224 |
| Max. dry density, $\rho_{d(\max)}$ (KN/m ³) | 16,36 | 14,38 | 18,12 | 14,83 | JIS A 1224 |
| Min. dry density, $\rho_{d(\min)}$ (KN/m ³) | 13,40 | 11,73 | 13,97 | 11,68 | JIS A 1224 |

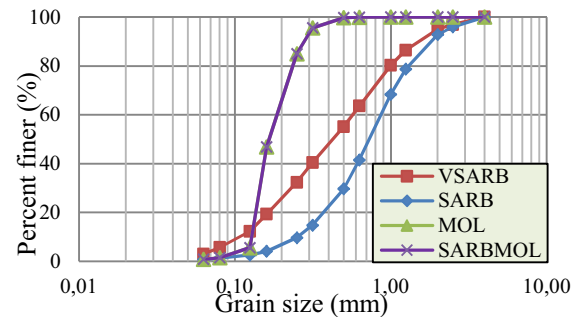


Figure 1. Grain size distribution curves of the studied materials

2.2. Test procedure

The triaxial samples, 50 mm in diameter and 90 mm in height, are prepared in five layers by using moist tamping based on the under-compaction method developed by Ladd 1978. However, instead of tamping on each layer, samples are hit by a plastic hammer at the sideways of the mount while the surface of each layer is being constrained by a solid plastic cylinder. This technique prevents the crushing of materials during sample preparation to get the target initial relative densities for the samples of 15%, 40% and 60%.

The samples are saturated by first flushing carbon dioxide (CO_2) to remove air. Subsequently deaired water is allowed to flow in the samples during 1 hour. After water flushing, the samples are loaded at 15 kPa cell pressure and 10 kPa back pressure. A differential pressure between cell pressure and back pressure is set to 5kPa and the saturation degree of the samples is checked by increasing the cell pressure and back pressure in three consecutive steps (30-25, 60-55, 105-100 kPa). All samples are considered to be fully saturated when the Skempton pore pressure ratio equals 0,95. Each sample is consolidated for 20 minutes until the volume change of the sample becomes stable, then bender element tests are performed at the target effective confining stresses of 25, 50, 75, 100, 125, 150, 175, 200, 225, 250, 275, 300 kPa. The change of void ratio of the samples at different effective confining pressure is measured using an external and local strain transducers and shown in Figure 3. In addition, measurements of the volume change are considered for validation only. Table 2 summarises the test series.

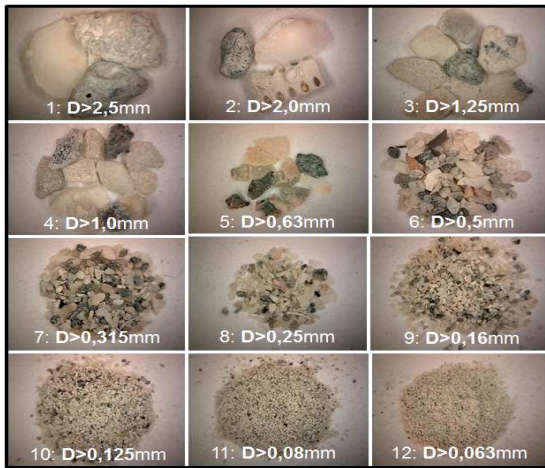


Figure 2. Microscopic views of different grain sizes of the Sarb sand bigger than 63µm

For the bender element test, a single sinusoidal pulse wave ($\pm 2V$ at 10kHz) is generated by a Picoscope. The method of first arrival time is used to obtain the travel time from transmitter to receiver combined with a stacking technique used in the studies of Santamarina & Fratta 2005 and Brandenburg et al. 2008. In this technique, a prescribed number of output wave signals are recorded and averaged for determining the travel time.

Table 2. Summary of the conducted isotropic consolidation tests with shear wave velocity measurement

| Test No. | Name of test | Initial relative density, D_r (%) | Confining effective stress, σ'_c (Kpa) |
|----------|--------------|-------------------------------------|---|
| 1 | Mol_Dr15 | 15 | 25 - 300 |
| 2 | Mol_Dr40 | 40 | 25 - 300 |
| 3 | Mol_Dr60 | 60 | 25 - 300 |
| 4 | Sarb_Dr15 | 15 | 25 - 300 |
| 5 | Sarb_Dr40 | 40 | 25 - 300 |
| 6 | Sarb_Dr60 | 60 | 25 - 300 |
| 7 | VSarb_Dr15 | 15 | 25 - 300 |
| 8 | VSarb_Dr40 | 40 | 25 - 300 |
| 9 | VSarb_Dr60 | 60 | 25 - 300 |
| 10 | SarbMol_Dr15 | 15 | 25 - 300 |
| 11 | SarbMol_Dr40 | 40 | 25 - 300 |
| 12 | SarbMol_Dr60 | 60 | 25 - 300 |

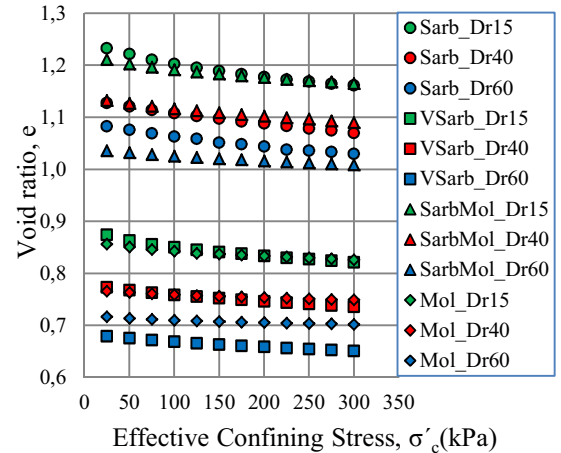


Figure 3. Void ratio of the samples versus effective confining stress.

3. TEST RESULTS AND DISCUSSION

Figure 4 and Figure 5 show the measured G_{max} versus the effective confining pressure p' and versus void ratio e for all tested materials at different initial relative densities. It can be seen that G_{max} increases with confining pressure and decreases with void ratio. The data of all tests are least-square fitted to estimate the material constants A , B (Lo presti), n listed in Table 3 so G_{max} can be predicted by Eq. (1).

Table 3, the values of the constants A , B , n for all sands were plotted versus the coefficient of uniformity C_u in Figure 6. This figure shows that the specimens having the same particles give an increase in A with increasing C_u ($C_{uSarb} = 3,46$, $C_{uSarbMol} = 1,44$). However, VSarb shows a decrease in A compared to Sarb and SarbMol. It is possible to say that after crushing the angularity of the particles decreases and so A decreases.

The value A of the two sands SarbMol and Mol with equal C_u increases with increasing angularity of the particles (SarbMol sand shows more angular particles than Mol sand). This effect is observed in specimens prepared at low and high relative densities. Besides the shape and angularity of the grains (Cho et al. 2006), the hardness of the particles can also be taken into account. This indicates that there is less dynamic stiffness in

silica sand (Mol sand) in comparison with calcareous sand.

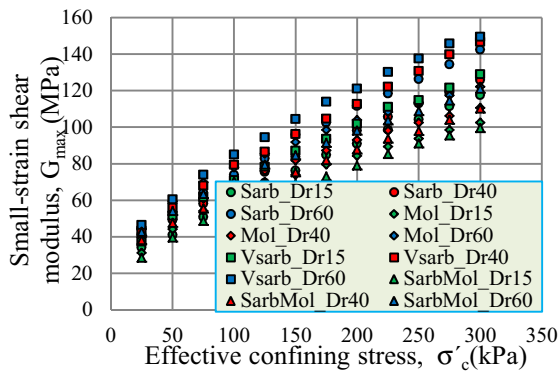


Figure 4. Increase of G_{\max} with confining pressure p'

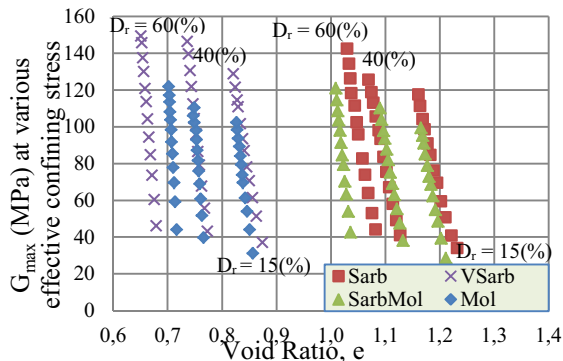


Figure 5. Decrease of G_{\max} with void ratio e at various effective confining stresses

Table 3. Material constants

| Sand type | A | B | n | R^2 | C_u | Range of e |
|-----------|--------|-------|-------|--------|-------|--------------|
| Sarb | 82,327 | 1,618 | 0,5 | 0,9883 | 3,46 | 0,903-1,33 |
| Vsarb | 63,658 | 0,721 | 0,504 | 0,9938 | 5,249 | 0,508-0,956 |
| SarbMol | 73,587 | 1,443 | 0,448 | 0,994 | 1,44 | 0,843-1,340 |
| Mol | 49,767 | 1,23 | 0,413 | 0,9953 | 1,44 | 0,581-0,93 |

The value of the exponent n varies between 0.41 for silica sand (Mol sand) and 0.44 - 0.51 for calcareous sand (Figure 6c). These values are close to 0.5 as proposed by Hardin & Richart (1963) (cited in Iwasaki & Tatsuoka 1977) and are in good agreement with the values obtained by many other authors on different sands (Delfosse-Ribay et

al. 2004, Hoque & Tatsuoka 2004, Santamarina & Cho 2004, Bui et al. 2007, Wichtmann & Triantafyllidis 2009). The trend of the parameter B is quite similar to A as shown in Figure 6b.

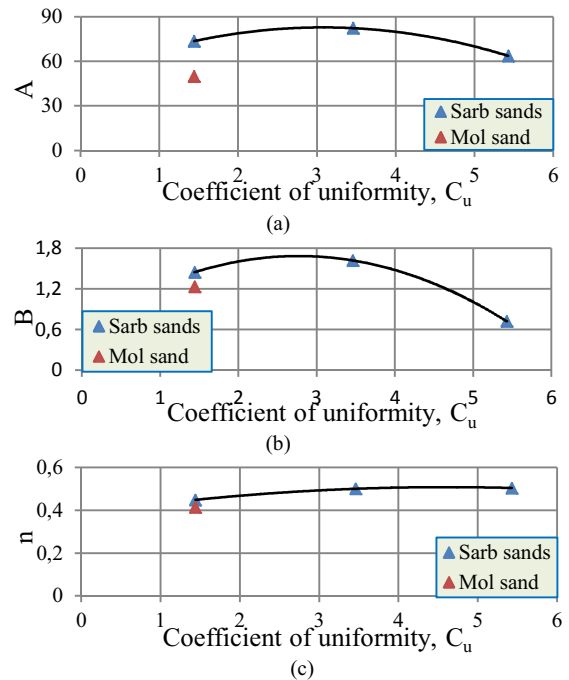


Figure 6. Material constants A, B, and n in function of C_u for calcareous sands and Mol sand

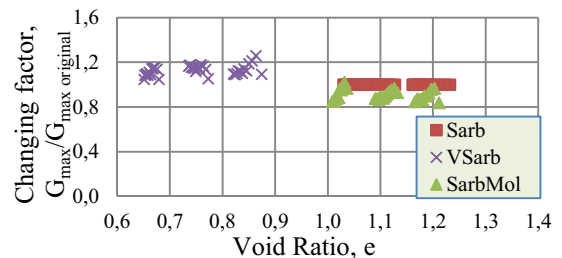


Figure 7. G_{\max} of manipulated sands compared to the original Sarb sand

In order to visualize the effect of GSD on G_{\max} , the results are expressed in terms of the ratio of G_{\max} of the manipulated calcareous sands to G_{\max} of the original calcareous sand, $G_{\max}/G_{\max \text{ original}}$ (Figure 7). Since two manipulated sands (Vsarb, sarbMol) are considered this ratio varies between 0.82 and 1.3. The shear modulus G_{\max} increases 25% after crushing for the Vsarb sand ($C_u=5,429$) and decreases 18% for the SarbMol sand

($C_u=1.44$). These differences in G_{max} are obviously due to the differences in GSD and void ratio expressed by the constants A and B. The influence of the void ratio is confirmed by Iwasaki & Tatsuoka (1977). Hardin & Drnevich (1972b) (cited in Bui et al. 2007) stated that the particle characteristics only change the void ratio and classified particle characteristics as relatively unimportant parameters for the assessment of the shear modulus. However, it is shown here, by comparison of the results for the Sarb, VSarb and SarbMol sands that particle characteristics do have an influence on G_{max} .

4. CONCLUSIONS

Based on the test results obtained, the following observations are made:

Shear modulus G_{max} cannot be predicted via mean effective stress p' alone. G_{max} increases with confining pressure and decreases with void ratio.

Particle shape and angularity of grains affect the shear modulus G_{max} when comparing silica and calcareous sands. For constant C_u the shear modulus of the calcareous sands is higher than that of silica sand.

GSD is an important parameter to evaluate G_{max} of soils. Crushable sands often have well graded classification while non-crushable sands like silica sand are poorly graded. Specimens having the same particles give an increase in A with increasing C_u .

Due to the limited test series, correlations of the material constants with C_u to predict G_{max} could not be developed in the current study.

REFERENCES

- Bellotti, R., Jamiolkowski, M., Presti, D.C.F.L. & O'Neill, D.A. 1996. Anisotropy of small strain stiffness in Ticino sand. *Geotechnique* 46, 115-131.
- Brandenberg, S.J., Kutter, B.L. and Wilson, D.W. 2008. Fast stacking and phase corrections of shear wave signals in a noisy environment. *Journal of Geotechnical and Geoenvironmental Engineering* 134, 1154-1165.
- Bui, M. T., Clayton, C. & Priest, J.A. 2007. Effects of particle shape on G_{max} of geomaterials. 4th International Conference on Earthquake Geotechnical Engineering.
- Builes, M., García, E. & Riveros, C.A. 2008. Dynamic and static measurements of small strain moduli of toyoura sand. *Revista Facultad de Ingeniería Universidad de Antioquia*(43), 86-101.
- Cho, G.-C., Dodds, J. & Santamarina, J.C. 2006. Particle shape effects on packing density, stiffness, and strength: natural and crushed sands. *Journal of Geotechnical and Geoenvironmental Engineering* 132, 591-602.
- Datta, M., Rao, G. & Gulhati, S. 1982. Engineering Behavior of Carbonate Soils of India and Some Observations on Classification of Such Soils. Geotechnical Properties, Behavior, and Performance of Calcareous Soils. K. Demars and R. Chaney, American Society for Testing and Materials. ASTM Special Technical Publication 777: 113-140.
- Delfosse-Ribay, E., Djeran-Maigre, I., Cabrillac, R. & Gouvenot, D. 2004. Shear modulus and damping ratio of grouted sand. *Soil Dynamics and Earthquake Engineering* 24, 461-471.
- Hoque, E. & Tatsuoka, F. 2004. Effects of stress ratio on small-strain stiffness during triaxial shearing. *Géotechnique* 54, 429-439.
- Hyodo, M., Aramaki, N. Itoh, M. & Hyde, A.F. 1996. Cyclic strength and deformation of crushable carbonate sand. *Soil Dynamics and Earthquake Engineering* 15, 331-336.
- Iwasaki, T. & Tatsuoka, F. 1977. Effects of grain size and grading on dynamic shear moduli of sands. *Japanese Society of Soil Mechanics and Foundation Engineering* 17, 19-35.
- Ladd, R. 1978. Preparing test specimens using undercompaction. *ASTM Geotechnical Testing Journal* 1.
- Maheswari, R. U., Boominathan, A. & Dodagoudar, G. 2008. Low strain shear modulus from field and laboratory tests. *Earthquake Hazards and Mitigation*, 415.
- Menq, F.-Y., Stokoe, K. Di Benedetto, H. Doanh, T. Geoffroy, H. & Sauzéat, C. 2003. Linear dynamic properties of sandy and gravelly soils from large-scale resonant tests, Swets & Zeitlinger Lisse, Netherlands.
- Sandoval, E.A. & Pando, M.A. 2012. Experimental assessment of the liquefaction resistance of calcareous biogenous sands. *Earth Sciences Research Journal* 16.
- Santamarina, J. & Cho, G. 2004. Soil behaviour: The role of particle shape. *Advances in Geotechnical Engineering: The Skempton Conference*, Thomas Telford.
- Santamarina, J. C. & Fratta, D. 2005. *Discrete signals and inverse problems: an introduction for engineers and scientists*, Wiley.
- Santos, J. & Gomes Correia, A. 2000. Shear modulus of soils under cyclic loading at small and medium strain level. *Proceedings, 12th World Conf. Earthquake Eng.*
- Towhata, I. 2008. *Geotechnical earthquake engineering*, Springer.
- Wichtmann, T. & Triantafyllidis, T. 2009. Influence of the grain-size distribution curve of quartz sand on the small strain shear modulus G_{max} . *Journal of Geotechnical and Geoenvironmental Engineering* 135, 1404-1418.
- Yang, J. & Gu, X. 2013. Shear stiffness of granular material at small strains: does it depend on grain size? *Géotechnique* 63, 165-179.